Journal of Physics: Conference Series **68** (2007) 012005 doi:10.1088/1742-6596/68/1/012005

Accelerating Universe and Scalar-Tensor Theories

Leandros Perivolaropoulos

University of Ioannina, Physics Department
Theoretical Physics Division
Ioannina, Greece

E-mail: leandros@uoi.gr

Abstract. Observational probes of dark energy converge on the fact that its equation of state w is close to -1. Some of these probes (for example the Gold SnIa sample) mildly support the possibility that w is time dependent and crosses the phantom divide line $w = -1$. Such a crossing is inconsistent with dark energy in the form of a single minimally coupled scalar field for any form of the field Lagrangian. The simplest theoretically motivated theories that are consistent with such crossing of the phantom divide are scalar-tensor extensions of general relativity. Therefore the crossing of the phantom divide if confirmed by future observations could be viewed as an indication hinting towards extensions of general relativity. Alternative signatures of extended gravity theories can be traced in the growth rate of density perturbations at recent redshifts as observed recently by the 2dFGRS.

1. Introduction

The assumption of large scale homogeneity and isotropy of the universe combined with the assumption that general relativity is the correct theory on cosmological scales leads to the Friedman equation which in a flat universe takes the form

$$H^2(a) = \left(\frac{\dot{a}}{a}\right)^2 = \frac{8\pi G}{3}\rho(a) \tag{1}$$

where $a(t)$ is the scale factor of the universe and ρ its average energy density. Both sides of this equation can be observationally probed directly: The left side using mainly geometrical methods (measuring the luminosity and angular diameter distances $d_L(z)$ and $d_A(z)$) showing an accelerating expansion at recent redshifts [1] and the matter - radiation density part of the right side using dynamical and other methods (cosmic microwave background [2], large scale structure observations [3], lensing [4] etc). These observations have indicated that the two sides of the Friedman equation (1) can not be equal if $\rho(a) = \rho_m(a) \sim a^{-3}$ even if a non-zero curvature is assumed. There are two possible resolutions to this puzzle: Either modify the right side of the Friedman equation (1) introducing a new form of *'dark' energy* component ($\rho(a) = \rho_m(a) + \rho_X(a)$) with suitable evolution in order to restore the equality or modify

both sides by changing the way energy density affects geometry thus modifying the Einstein equations.

In the first class of approaches the required gravitational properties of dark energy needed to induce the accelerating expansion are well described by its equation of state $w(z) = \frac{p_X(z)}{\rho_X(z)}$ which enters in the second Friedman equation as

$$\frac{\ddot{a}}{a} = -\frac{4\pi G}{3}(\rho_m + \rho_X(1+3w)) \tag{2}$$

implying that a negative pressure ($w < -1/3$) is necessary in order to induce accelerating expansion. The simplest viable example of dark energy is the cosmological constant[5] ($w = -1$). This example however even though consistent with present data lacks physical motivation. Questions like 'What is the origin of the cosmological constant?' or 'Why is the cosmological constant 10^{120} times smaller than its natural scale so that it starts dominating at recent cosmological times (coincidence problem)?' remain unanswered. Attempts to replace the cosmological constant by a dynamical scalar field (quintessence[6]) have created a new problem regarding the initial conditions of quintessence which even though can be resolved in particular cases (tracker quintessence), can not answer the above questions in a satisfactory way.

The parameter $w(z)$ determines not only the gravitational properties of dark energy but also its evolution. This evolution is easily obtained from the energy momentum conservation

$$d(\rho_X a^3) = -p_X d(a^3) \tag{3}$$

which leads to

$$\rho_X = \rho_{0X} e^{-3\int_1^a \frac{da'}{a'}(1+w(a'))} = \rho_{0X} e^{-3\int_0^z \frac{dz'}{1+z'}(1+w(z'))} \tag{4}$$

Therefore the determination of $w(z)$ is equivalent to that of $\rho_X(z)$ which in turn is equivalent to the observed $H(z)$ from the Friedman equation (1) which may be written as

$$H(z) = H_0(\Omega_{0\mathrm{m}}(1+z)^3 + \Omega_{0X} e^{-3\int_0^z \frac{dz'}{1+z'}(1+w(z'))}) \tag{5}$$

Thus, knowledge of $\Omega_{0\mathrm{m}}$ and $H(z)$ suffices to determine $w(z)$ which is obtained from equation (5) as

$$w(z) = \frac{\frac{2}{3}(1+z)\frac{dlnH}{dz} - 1}{1 - \frac{H_0^2}{H^2}\Omega_{0\mathrm{m}}(1+z)^3} \tag{6}$$

In the second class of approaches the Einstein equations get modified and the new equations combined with the assumption of homogeneity and isotropy lead to a generalized Friedman equation of the form

$$f(H^2) = g(\rho_m) \tag{7}$$

where f and g are appropriate functions determined by the modified gravity theory[7]. In this class of models, the parameter $w(z)$ can also be defined from equation (6) but it can not be interpreted as $\frac{p_X}{\rho_X}$ of a perfect fluid.

The first step towards understanding the gravitational properties of dark energy or distinguishing between the two classes of theories is the measurement of the Hubble expansion history $H(z)$ at recent redshifts. A particularly useful tool for this purpose is the *Hubble diagram*.

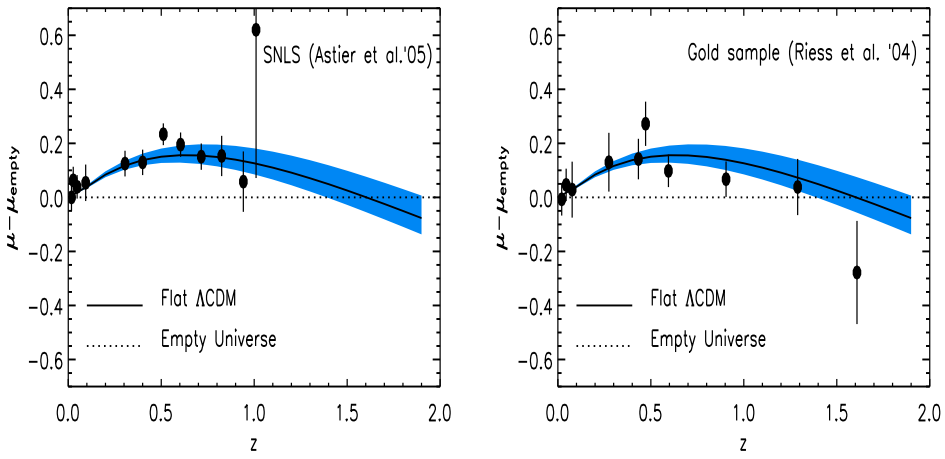

Figure 1. The distance modulus of the SnIa data normalized on that of an empty universe ($H(z) = H_0$) versus redshift (in redshift bins) for the SNLS and Gold datasets. The best fit ΛCDM to WMAP-3 is also shown (from Ref. [2])

The luminous objects used in the construction of the Hubble diagram are objects whose absolute luminosity is known and therefore their distance can be evaluated from their apparent luminosity along the lines discussed above. Such objects are known as *distance indicators* or *standard candles*. The best choice distance indicators for cosmology are SnIa not only because they are extremely luminous (at their peak they are as luminous as a bright galaxy) but also because their absolute magnitude can be determined at a high accuracy.

The two deepest (in redshift space) and reliable datasets for the construction of the Hubble diagram are the Gold sample and the first year Supernova Legacy Survey sample (Fig. 1). The Gold sample consisting of 157 points extends in redshift space in the range $0 < z < 1.7$ while the SNLS dataset extends in the range $0 < z < 1$. The Hubble diagram obtained from each sample is shown in Fig. 1. The data of Fig. 1 are binned in redshift bins and the vertical axis shows the distance modulus (proportional $log_{10}(d_L(z))$ of the SnIa data normalized on that of an empty universe with $H(z) = H_0 = constant$. In such a diagram a positive slope corresponds to an accelerating universe while a negative slope corresponds to a decelerating universe. The best fit curve obtained from the WMAP CMB perturbation spectrum (location of the first peak) is also shown for comparison (from Ref. [2]). Clearly both plots indicate that the universe is currently accelerating and that this acceleration started at $z \simeq 0.5$. The Hubble expansion history can be obtained by differentiating the observed luminosity distance $d_L(z)$ as

$$\left(\frac{\dot{a}}{a}\right)(z) = H(z) = \frac{1}{c}\left[\frac{d}{dz}\left(\frac{d_L(z)}{1+z}\right)\right]^{-1} \tag{8}$$

where we have assumed flatness. The best fit form of $H(z)$ as obtained from the SnIa data and other dark energy probes will be outlined in the next section.

2. Best Fits for H(z)-w(z)

The simplest $H(z)$ parametrization consistent with an accelerating expansion of the universe corresponds to the cosmological constant (LCDM) which in a general FRW spacetime is expressed as

$$H(z)^2 = H_0^2(\Omega_{0\mathrm{m}}(1+z)^3 + \Omega_\Lambda + \Omega_k(1+z)^2) \tag{9}$$

where $\Omega_{0\mathrm{m}} + \Omega_\Lambda + \Omega_k = 1$ and $H_0^2\Omega_k(1+z)^2 = \frac{k}{a^2}$ represents a non-zero curvature of the universe.

SnIa observations provide the apparent luminosity $l(z)$ for each SnIa while the absolute luminosity L is assumed to be the same for all SnIa (after the appropriate corrections on $l(z)$). The luminosities $l(z)$ and L are connected to the apparent and absolute magnitudes $m(z)$ and M and with the observed luminosity distance $d_L(z)$ as

$$2.5log_{10}\left(\frac{L}{l(z)}\right) = \mu = m(z) - M - 25 = 5log_{10}\left(\frac{d_L(z)_{obs}}{Mpc}\right) \tag{10}$$

The corresponding theoretical prediction given the $H(z)$ ansatz of equation (9) is of the form

$$d_L(z)_{th} = \frac{c(1+z)}{H_0\sqrt{\Omega_{0\mathrm{m}} + \Omega_\Lambda - 1}} \sin\left[\sqrt{\Omega_{0\mathrm{m}} + \Omega_\Lambda - 1}\int_0^z \frac{H_0 dz'}{H(z';\Omega_{0\mathrm{m}},\Omega_\Lambda)}\right] \tag{11}$$

which in the flat case $\Omega_{0\mathrm{m}} + \Omega_\Lambda = 1$ reduces to equation (8). In order to find the best fit parameter values $\Omega_{0\mathrm{m}}$, Ω_Λ we can minimize

$$\chi^2(\Omega_{0\mathrm{m}},\Omega_\Lambda) = \sum_{i=1}^{N} \frac{[5log_{10}(d_L(z_i)_{obs}) - 5log_{10}(d_L(z_i;\Omega_{0\mathrm{m}},\Omega_\Lambda)_{th})]^2}{\sigma_i^2} \tag{12}$$

The resulting $\chi^2(\Omega_{0\mathrm{m}},\Omega_\Lambda)$ contours [8] using the Gold and SNLS datasets indicate the following:

- Both datasets rule out a flat matter dominated universe with $\Omega_{0\mathrm{m}} = 1$ at about 10σ level.
- The Gold dataset mildly favors a closed universe over flat LCDM ($\Omega_\Lambda = 0.98 \pm 0.30$, $\Omega_{0\mathrm{m}} = 0.46 \pm 0.14$) while the best fit of SNLS almost coincides with flat LCDM ($\Omega_\Lambda = 0.78 \pm 0.31$, $\Omega_{0\mathrm{m}} = 0.29 \pm 0.21$) [8].
- The two datasets are consistent with each other at the 2σ level.

Despite the fact that flat LCDM is consistent with current SnIa data, it is interesting to investigate how much can we improve the quality of fit to the data by adding one or two parameters. To address this question we can follow the following strategy

(i) Consider a n parameter parametrization $H(z;a_1,...,a_n)$ which may be either motivated by a physical model or be arbitrary, designed to provide the best fit to the data.

(ii) Assuming flatness, obtain the theoretical prediction of the luminosity distance from this parameterization

$$d_L(z)_{th} = c(1+z)\int_0^z \frac{dz'}{H(z';a_1,...,a_n)} \tag{13}$$

(iii) Use the observed luminosity distances to construct $\chi^2(a_1,...,a_n)$ along the lines of equation (12) and minimize with respect to the parameters $a_1,...,a_n$.

(iv) Compare the minimum value of χ^2 (χ^2_{min}) with the corresponding value obtained with different parametrizations thus finding the more efficient direction in functional space to decrease χ^2_{min}.

The same strategy can be followed using alternative to SnIa dark energy probes like the shift parameter [9, 10]

$$R = \Omega_{0\mathrm{m}}^{1/2}\int_0^{z_{rec}} \frac{dz'}{E(z')} = 1.70 \pm 0.03 \tag{14}$$

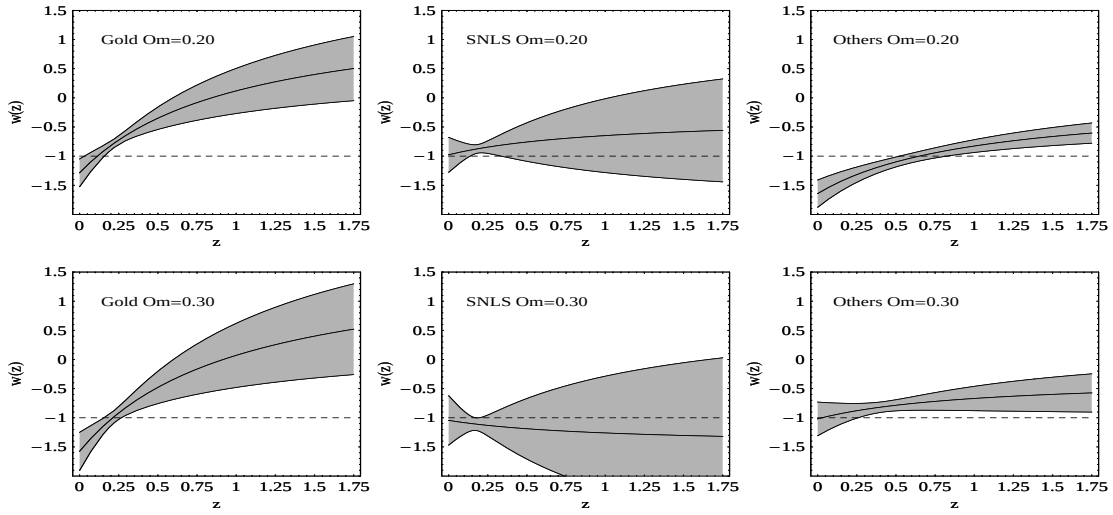

Figure 2. The best fit $w(z)$ for three classes of data (upper row $\Omega_{0\mathrm{m}} = 0.2$, lower row $\Omega_{0\mathrm{m}} = 0.3$).

the A parameter of the baryon acoustic oscillations peak

$$A = \sqrt{\Omega_{0\mathrm{m}}} E(z_1)^{-1/3} [\frac{1}{z_1} \int_0^{z_1} \frac{dz'}{E(z')}]^{2/3} = 0.469 \pm 0.017 \tag{15}$$

where $E(z) \equiv H(z)/H_0$, the cluster gas baryon fraction [11] and the growth rate of perturbations at $z = 0.15$ as obtained from the 2dFGRS [12].

Along the lines of the above approach, the matter density $\Omega_{0\mathrm{m}}$ appears as a nuisance parameter which can be either marginalized over an observationally preferred range (eg $\Omega_{0\mathrm{m}} \in [0.2, 0.3]$) or fixed to a set of values consistent with other observations in order to identify the dependence of the dark energy properties on this parameter. Here we have followed the later approach and considered the values $\Omega_{0\mathrm{m}} = 0.2$, $\Omega_{0\mathrm{m}} = 0.3$ in the context of the parametrization [13, 14]

$$w(z) = w_0 + w_1 \frac{z}{1+z} \tag{16}$$

The corresponding form of $H(z)$ assuming flatness is obtained using equation (6) as

$$\begin{aligned} H^2(z) &= H_0^2 [\Omega_{0m}(1+z)^3 + \\ &+ (1-\Omega_{0m})(1+z)^{3(1+w_0+w_1)} e^{3w_1[1/(1+z)-1]}] \end{aligned} \tag{17}$$

The best fit form of $w(z)$ for three classes of data is shown in Fig. 2. The first column corresponds to the Gold dataset and shows the mild trend for an evolving $w(z)$ crossing the phantom divide line (PDL) $w = -1$ for both values of $\Omega_{0\mathrm{m}}$. The second column corresponds to the SNLS data and shows no trend for an evolving $w(z)$ for any value of $\Omega_{0\mathrm{m}}$. Instead, the best fit $w(z)$ is very close to $w = -1$. The third column of Fig. 2 corresponds to other than SnIa dark energy probes including the 3-year WMAP CMB shift parameter [9], the BAO peak from SDSS [15], the Cluster gas mass fraction [11] and the growth rate $g(z)$ of matter perturbations at $z = 0.15$ from 2dFGRS ($g(z = 0.15) = \frac{dlnD(a)}{dlna} = 0.51 \pm 0.11$) [16]. These data which are dominated by the CMB-BAO part (having the smallest relative errors) favor a crossing of the PDL only for low values of $\Omega_{0\mathrm{m}}$ ($\Omega_{0\mathrm{m}} < 0.25$). It is clear from Fig. 2 that all currently available

cosmological data favor a $w \simeq -1$ while some dark energy probes mildly favor an evolving $w(z)$ crossing the PDL. It is therefore important to address the following question: *What theories are consistent with the crossing of the PDL $w = -1$?*

3. Phantom Divide Crossing and Extended Gravity Theories

The simplest model predicting an evolving $w(z)$ is a model where the role of dark energy is played by a minimally coupled scalar field Φ whose dynamics is determined by a potential $V(\Phi)$. The Lagrangian density for such a field is of the form

$$\mathcal{L} = \pm\frac{1}{2}\dot{\Phi}^2 - V(\Phi) \tag{18}$$

where the upper (+) sign refers to quintessence while the lower (-) sign corresponds to a phantom[17] scalar field. The equation of state for such a system is of the form

$$w \equiv \frac{p}{\rho} = \frac{\pm\frac{1}{2}\dot{\Phi}^2 - V(\Phi)}{\pm\frac{1}{2}\dot{\Phi}^2 + V(\Phi)} \tag{19}$$

For a small kinetic term ($\dot{\Phi} \to 0$) we get $w \to -1$ and we reobtain the cosmological constant. For $\dot{\Phi} \neq 0$ the parameter w remains larger (smaller) than -1 for the quintessence (phantom) case (assuming $V(\Phi) > 0$). Clearly therefore neither the phantom nor the quintessence case can cross the PDL $w = -1$ since that would require changing the sign of the kinetic term $\dot{\Phi}^2$. This however is impossible for a real scalar field. Therefore, a minimally coupled scalar field is inconsistent[18] with crossing the PDL $w = -1$. This result has been generalized by Vikman[19] to the case of k-essence[20] ie a generalized minimally coupled scalar field Lagrangian which depends on $\dot{\Phi}^2$ in an arbitrary way.

In principle, a combination of quintessence + phantom scalar field could lead to a multi-component dark energy system dynamically leading to crossing of the PDL[21]. However, such a system is plagued with severe instabilities at the quantum (and even the classical) level due to the fact that its energy is unbounded from below[22]. Therefore, as discussed below, the simplest theoretically motivated models consistent with crossing of the PDL are scalar-tensor extensions of general relativity.

In these theories Newton's constant obtains dynamical properties expressed through the potential $F(\Phi)$. The dynamics are determined by the Lagrangian density[23]

$$\mathcal{L} = \frac{F(\Phi)}{2}\, R - \frac{1}{2}\, g^{\mu\nu}\partial_\mu\Phi\partial_\nu\Phi - U(\Phi) + \mathcal{L}_m[\psi_m; g_{\mu\nu}] \ . \tag{20}$$

where $\mathcal{L}_m[\psi_m; g_{\mu\nu}]$ represents matter fields approximated by a pressureless perfect fluid. The function $F(\Phi)$ is observationally constrained as follows:

- $F(\Phi) > 0$ so that gravitons carry positive energy.
- $\frac{dF}{d\Phi} < 10^{-5}$ from solar system observations.

Assuming a homogeneous Φ and varying the action corresponding to (20) in a background of a flat FRW metric, we find the coupled system of generalized Friedman equations

$$3FH^2 = \rho + \frac{1}{2}\dot{\Phi}^2 - 3H\dot{F} + U \tag{21}$$

$$-2F\dot{H} = \rho + p + \dot{\Phi}^2 + \ddot{F} - H\dot{F} \tag{22}$$

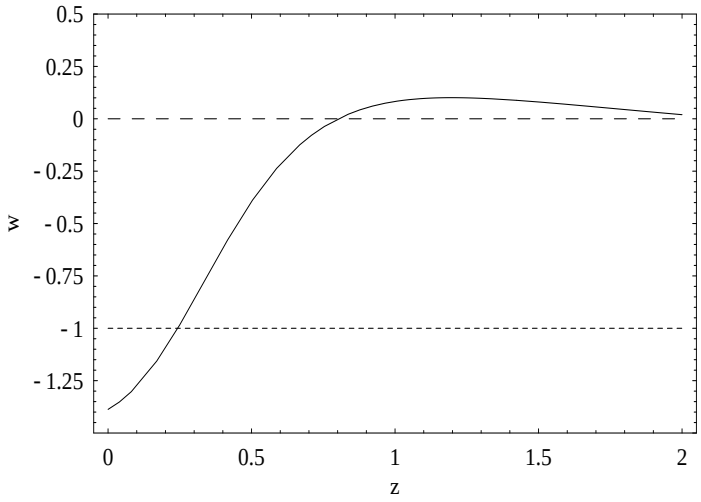

Figure 3. The form of $w(z)$ used for the reconstruction of the scalar-tensor theory.

where we have assumed the presence of a perfect fluid ($\rho, p \simeq 0$) playing the role of matter fields. These equations reduce as expected to the ordinary Friedman equations by setting $F = \frac{1}{8\pi G} = constant$. It is clear from equation (22) that a properly chosen $F(t) \sim G(t)^{-1}$ can boost the accelerating expansion which in general relativity is induced solely by the field potential U (for a more extensive discussion on this see Ref. [24]). On the other hand, the kinetic term $\dot{\Phi}^2$ plays an attractive role that can only decrease the acceleration. The system (21), (22) can be used to reconstruct[25, 24, 26] the scalar-tensor theory (defined by $F(\Phi)$, $U(\Phi)$) using the observed $H(z)$, $\Omega_{0\mathrm{m}}$ (ρ_m). Unfortunately, this reconstruction involves three unknown functions ($\dot{\Phi}(t)$, $U(t)$, $F(t)$) with only two equations. This however is not a problem if our goal is not the unique reconstruction of the scalar-tensor theory but the proof of the *existence* of an $F(\Phi)$, $U(\Phi)$ that can reproduce an $H(z)$ crossing the PDL $w = -1$. By expressing the system (21), (22) in redshift space (instead of time) and using an ansatz for a small $\Phi'(z)$ it is straightforward [24] to solve for $F(\Phi)$, $U(\Phi)$ using an $H(z)$ that corresponds to crossing the PDL. The input $w(z)$, obtained from a polynomial parametrization of $H(z)$ fitted to the Gold dataset, is shown in Fig. 3. The resulting $F(\Phi)$, $U(\Phi)$ are shown in Fig. 4 which assumes $\Phi(z = 0) = 0$. From Fig. 4b it is clear that F increases with time at recent redshifts which implies that $G \sim F^{-1}$ decreases with time thus boosting the accelerating expansion and allowing the crossing of $w = -1$ which would be impossible by utilizing only the gravitationally repulsive potential U [24]. It is therefore clear that the crossing of the PDL is possible in scalar-tensor theories which makes them prime candidate theories if such crossing is observed in the future.

4. Alternative Signatures

An alternative signature of extended gravity theories is provided by a dynamical probe of geometry which is the measured linear growth factor of the matter density perturbations $D(a)$ defined as

$$D(a) \equiv \frac{\frac{\delta\rho}{\rho}(a)}{\frac{\delta\rho}{\rho}(a = 1)} \tag{23}$$

The measurements of $D(a)$ can be made by several methods including the redshift distortion factor in redshift surveys, weak lensing, number counts of galaxy clusters, Integrated Sachs-

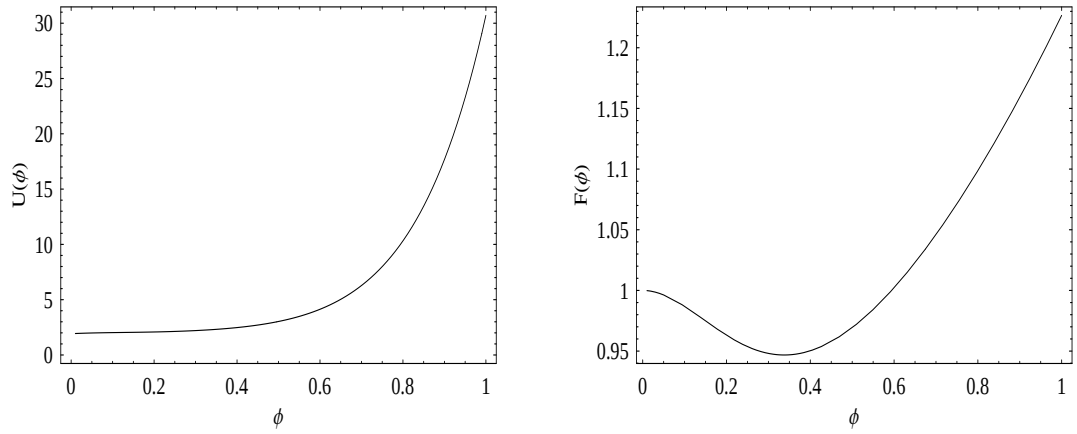

Figure 4. The reconstructed potentials $U(\Phi)$ and $F(\Phi)$.

Wolfe (ISW) effect and large scale structure power spectrum. The theoretical prediction of the evolution of $D(a)$ on sub-Hubble scales is obtained from the Euler and conservation equations as

$$D''(k,a) + (\frac{3}{a} + \frac{H'(a)}{H(a)})D'(k,a) - \frac{3}{2}\frac{\Omega_{0m}}{a^5 H(a)^2} f(k,a) D(k,a) = 0 \tag{24}$$

with initial conditions $D(a) \simeq a$ for $a \simeq 0$. In equation (24) we have ignored anisotropic stresses and dark energy perturbations which are expected to have a small effect on sub-Hubble scales. The last term of equation (24) emerges by connecting the metric perturbation with the matter density perturbations. It therefore depends on the particular form of the dynamical equations of the gravity theory considered. This dependence is expressed through the function $f(k,a)$ which in the case of general relativity is unity ($f(k,a) = 1$) while in extended gravity theories it can take values different from one which can even depend on the scale k. For example for scalar-tensor theories we have[25]

$$f(k,a) = \frac{G_{eff}(a)}{G_{eff}(a=1)}(1 + \frac{1}{1 + \frac{k}{ma}}) \simeq \frac{F_0}{F(a)} \tag{25}$$

where $G_{eff}(a)$ is the effective Newton's constant when the scale factor is a and $a = 1$ corresponds to the present value of the scale factor while m is the mass of the scalar field Φ inducing a Yukawa cutoff to the gravitational field. Also for the DGP model[28, 29] we have[30]

$$f(k,a) = (1 + \frac{1}{3\beta}) \tag{26}$$

with

$$\beta = 1 - \frac{H(a)}{H_0 \Omega_{r_c}}(1 + \frac{a}{3}\frac{H'(a)}{H(a)}) \tag{27}$$

where r_c is the crossover scale beyond which the gravitational force follows the 5-dimensional $1/r^3$ behavior and

$$\Omega_{r_c} \equiv 1/4 r_c^2 H_0^2 \tag{28}$$

The detection of an $f(k,a) \neq 1$ from equation (24) would therefore be a 'smoking gun' signature of extended gravity theories. Such a detection could be made for example by using the form

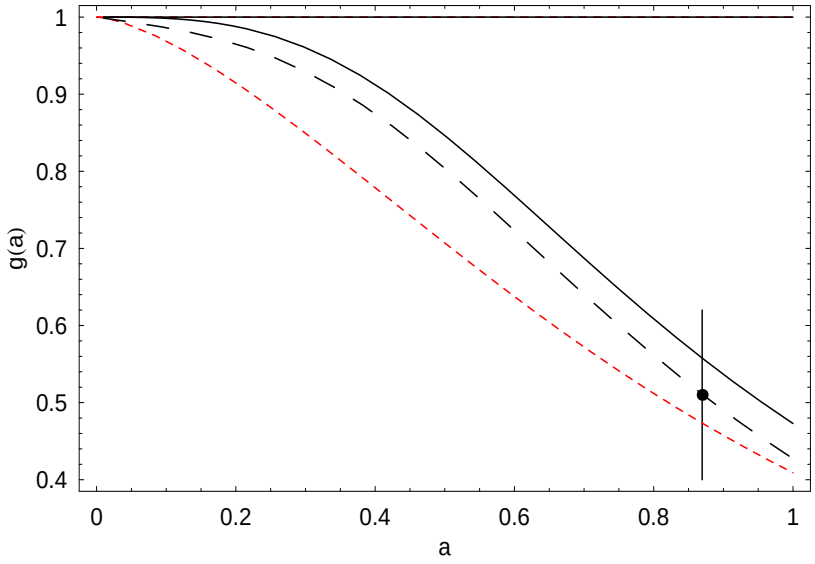

Figure 5. The growth rate of perturbations as a function of the scale factor for LCDM (continous line), the best fit to SnIa flat DGP model(short dashed line) and scalar tensor theories with a particular form Newton's constant evolution (long dashed line: $G(a) = G_0(1+(1-a)/2)$). The datapoint from 2dFGRS at $z = 0.15$ is also shown indicating consistency of all plotted theories with the current errorbars.

of $H(z)$ obtained from geometric tests in equation (24), solving for $D(a)$ in the context of general relativity ($f(k, a) = 1$) and comparing with the observed $D(a)$ at various redshifts. If a statistically significant difference is found between the observed $D(a)$ and one predicted in the context of general relativity then this could be interpreted as evidence for extensions of general relativity. There is currently an observational estimate of the growth rate defined as

$$g(a) \equiv \frac{aD'(a)}{D(a)} \tag{29}$$

at a redshift $z = \frac{1}{a} - 1 = 0.15$ from the 2dFGRS[12, 27] as

$$g(z = 0.15) = 0.51 \pm 0.11 \tag{30}$$

using the redshift distortion factor and there will soon be better estimates coming from the SDSS. As demonstrated in Fig. 5 however, the large errorbars in the currently available datapoint of equation (30) imply that the best fit LCDM model (flat $\Omega_\Lambda = 0.72$) is consistent with the current growth rate observations. Future observations however may decrease this errorbar thus either confirming general relativity or favoring extended gravity theories.

Acknowledgements
This work was supported by the program PYTHAGORAS-1 of the Operational Program for Education and Initial Vocational Training of the Hellenic Ministry of Education under the Community Support Framework and the European Social Fund.

References

[1] Riess A *et al* , Astron. J. **116**(1998), 1009; Perlmutter S J *et al* , Astroph. J. **517**(1999), 565; Bull.Am.Astron.Soc**29**(1997),1351; Tonry, J L *et al* , Astroph. J. **594**,(2003) 1; Barris, B *et al* , Astroph. J. **602**,(2004) 571; Knop R *et al* , Astroph. J. **598**,(2003) 102; A. G. Riess *et al.* [Supernova Search

Team Collaboration], Astrophys. J. **607**(2004), 665 [arXiv:astro-ph/0402512]; P. Astier *et al.*, Astron. Astrophys. **447**(2006), 31 [arXiv:astro-ph/0510447].
[2] D. N. Spergel *et al.*, "Wilkinson Microwave Anisotropy Probe (WMAP) three year results: arXiv:astro-ph/0603449.
[3] M. Tegmark *et al.* [SDSS Collaboration], Phys. Rev. D **69**(2004), 103501.
[4] N. Kaiser and G. Squires, Astrophys. J. **404**(1993), 441.
[5] V. Sahni and A. A. Starobinsky, Int. J. Mod. Phys. D **9**(2000), 373 [arXiv:astro-ph/9904398]; S. M. Carroll, Living Rev. Rel. **4**(2001), 1 [arXiv:astro-ph/0004075]; P. J. E. Peebles and B. Ratra, Rev. Mod. Phys. **75**(2003), 559 [arXiv:astro-ph/0207347]; T. Padmanabhan, Phys. Rept. **380**(2003), 235 [arXiv:hep-th/0212290].
[6] B. Ratra and P.J.E. Peebles, Phys. Rev. D**37**(1988), 3406; Rev. Mod. Phys. **75**(2003), 559 [arXiv:astro-ph/0207347]; C. Wetterich, Nucl. Phys. B **302**(1988), 668; P.G.Ferreira and M. Joyce, Phys. Rev. D.**58**(1998), 023503.
[7] B. Boisseau, G. Esposito-Farese, D. Polarski and A. A. Starobinsky, Phys. Rev. Lett. **85**(2000), 2236 [arXiv:gr-qc/0001066]; F. Perrotta, C. Baccigalupi and S. Matarrese, Phys. Rev. D **61**(2000), 023507 [arXiv:astro-ph/9906066];
[8] S. Nesseris and L. Perivolaropoulos, "Comparison of the Legacy and Gold SnIa Dataset Constraints on Dark Energy Phys. Rev. D **72**(2005), 123519 [arXiv:astro-ph/0511040].
[9] J. R. Bond, G. Efstathiou and M. Tegmark, "Forecasting Cosmic Parameter Errors from Microwave Background Anisotropy Mon. Not. Roy. Astron. Soc. **291**(1997), L33 [arXiv:astro-ph/9702100].
[10] Y. Wang and P. Mukherjee, arXiv:astro-ph/0604051.
[11] S. W. Allen, R. W. Schmidt, H. Ebeling, A. C. Fabian and L. van Speybroeck, "Constraints on dark energy from Chandra observations of the largest Mon. Not. Roy. Astron. Soc. **353**(2004), 457 [arXiv:astro-ph/0405340].
[12] L. Verde *et al.*, "The 2dF Galaxy Redshift Survey: The bias of galaxies and the density of the Mon. Not. Roy. Astron. Soc. **335**(2002), 432 [arXiv:astro-ph/0112161].
[13] M. Chevallier and D. Polarski, Int. J. Mod. Phys. D **10**(2001), 213 [arXiv:gr-qc/0009008].
[14] E. V. Linder, Phys. Rev. Lett. **90**(2003), 091301 [arXiv:astro-ph/0208512].
[15] D. J. Eisenstein *et al.* [SDSS Collaboration], "Detection of the Baryon Acoustic Peak in the Large-Scale Correlation Astrophys. J. **633**(2005), 560 [arXiv:astro-ph/0501171].
[16] Y. Wang and M. Tegmark, "Uncorrelated Measurements of the Cosmic Expansion History and Dark Energy from Supernovae," Phys. Rev. D **71**(2005), 103513 [arXiv:astro-ph/0501351].
[17] R. R. Caldwell, Phys. Lett. B **545**(2002), 23 [arXiv:astro-ph/9908168]; P. Singh, M. Sami and N. Dadhich, Phys. Rev. D **68**(2003), 023522 [arXiv:hep-th/0305110]; V. B. Johri, Phys. Rev. D **70**(2004), 041303 [arXiv:astro-ph/0311293]; B. McInnes, Nature of Dark Energy: Proc., ed by P. Brax, J. Martin, J.P. Uzan. p. 265, arXiv:astro-ph/0210321.
[18] L. Perivolaropoulos, Phys. Rev. D **71**(2005), 063503 [arXiv:astro-ph/0412308].
[19] A. Vikman, Phys. Rev. D **71**(2005), 023515 [arXiv:astro-ph/0407107].
[20] C. Armendariz-Picon, V. Mukhanov and P. J. Steinhardt, Phys. Rev. D **63**(2001), 103510 [arXiv:astro-ph/0006373]; R. J. Scherrer, Phys. Rev. Lett. **93**(2004), 011301 [arXiv:astro-ph/0402316].
[21] X. F. Zhang, H. Li, Y. S. Piao and X. M. Zhang, Mod. Phys. Lett. A **21**(2006), 231 [arXiv:astro-ph/0501652]; M. z. Li, B. Feng and X. m. Zhang, JCAP **0512**(2005), 002 [arXiv:hep-ph/0503268];B. Feng, X. L. Wang and X. M. Zhang, Phys. Lett. B **607**(2005), 35 [arXiv:astro-ph/0404224].
[22] J. M. Cline, S. Jeon and G. D. Moore, Phys. Rev. D **70**(2004), 043543 [arXiv:hep-ph/0311312]; R. V. Buniy and S. D. H. Hsu, Phys. Lett. B **632**(2006), 543 [arXiv:hep-th/0502203]; A. De Felice, M. Hindmarsh and M. Trodden, arXiv:astro-ph/0604154.
[23] G. Esposito-Farese and D. Polarski, Phys. Rev. D **63**(2001), 063504 [arXiv:gr-qc/0009034];
[24] L. Perivolaropoulos, JCAP **10**(2005), 001 arXiv:astro-ph/0504582.
[25] B. Boisseau, G. Esposito-Farese, D. Polarski and A. A. Starobinsky, Phys. Rev. Lett. **85**(2000), 2236 [arXiv:gr-qc/0001066].
[26] S. Tsujikawa, Phys. Rev. D **72**(2005), 083512 [arXiv:astro-ph/0508542].
[27] E. Hawkins *et al.*, "The 2dF Galaxy Redshift Survey: correlation functions, peculiar velocities Mon. Not. Roy. Astron. Soc. **346**(2003), 78 [arXiv:astro-ph/0212375].
[28] G. R. Dvali, G. Gabadadze and M. Porrati, Phys. Lett. B **484**(2000), 112 [arXiv:hep-th/0002190].
[29] C. Deffayet, Phys. Lett. B **502**(2001), 199 [arXiv:hep-th/0010186].
[30] K. Koyama and R. Maartens, JCAP **0601**(2006), 016 [arXiv:astro-ph/0511634].